Vol. 695: 157–171, 2022
https://doi.org/10.3354/meps14123

MARINE ECOLOGY PROGRESS SERIES
Mar Ecol Prog Ser

Published August 25

Giant appetites: exploring the trophic ecology of California's largest kelp forest predator, the giant sea bass *Stereolepis gigas*

Kayla M. Blincow[1,2,*], Rasmus Swalethorp[1], Arturo Ramírez-Valdez[1,3,4], Brice X. Semmens[1]

[1]Scripps Institution of Oceanography, University of California, San Diego, La Jolla, California 92093, USA
[2]Center for Marine and Environmental Science, University of the Virgin Islands, St. Thomas, USVI 00802, USA
[3]Proyecto Mero Gigante - Giant Sea Bass Project, CP 22860 Ensenada, Baja California, Mexico
[4]Instituto de Investigaciones Oceanológicas, Universidad Autónoma de Baja California, CP 22860 Ensenada, Baja California, Mexico

ABSTRACT: The recovery of endangered predators has the potential to influence the ecosystems they inhabit. After suffering severe population declines due to fishing pressure, giant sea bass *Stereolepis gigas* in southern California, USA, are beginning to recover. As large-bodied predators often associated with the kelp forest and rocky reef environments of southern California and Baja California, Mexico, the local recovery of this species could influence trophic dynamics in these systems. Here we leverage stable isotope and gut content analysis to describe the trophic ecology of adult giant sea bass. We found that they are generalist predators, with larger individuals relying more heavily on macroalgae-derived carbon, occupying a larger trophic niche, and obtaining higher trophic positions. Using these results, we speculate about the relationship between giant sea bass and kelp forest ecosystems, a vulnerable yet key habitat, including the impact of the return of these predators, as well as how contemporary threats to kelp forests might mediate their continued recovery.

KEY WORDS: Stable isotopes · Endangered species · Gut contents · Feeding ecology · Generalist predator

1. INTRODUCTION

Many marine ecosystems have experienced declines in predator populations in recent decades (Heithaus et al. 2008, Ritchie & Johnson 2009, Sadovy de Mitcheson et al. 2013). Loss of top predators can result in trophic cascades (Heithaus et al. 2008, Donohue et al. 2017), disruption of nutrient cycling (Schmitz et al. 2010), and broader loss of biodiversity (Ritchie & Johnson 2009). In some cases, conservation and management action have been effective at supporting the recovery of depressed predator populations (Waterhouse et al. 2020). While this is a positive outcome, it can be difficult to predict how predator recovery will influence ecosystems that have been operating in their absence for decades or longer (Ritchie & Johnson 2009). One key component in understanding the implications of predator recovery is the trophic ecology of the predator in question. Understanding how predators fit into the trophic system (what they eat, which primary producers they rely on, etc.) can help assess the potential impacts of their return, as well as how prey and producer communities might mediate their continued recovery.

Giant sea bass *Stereolepis gigas* are Critically Endangered (Cornish 2004) large-bodied predators that

*Corresponding author: kaylamblincow@gmail.com

Publisher: Inter-Research · www.int-res.com

were once abundant in the kelp forests and rocky reefs of southern California, USA, and Baja California, Mexico (Dayton et al. 1998, Domeier 2001, Cornish 2004, Hawk & Allen 2014, Erauskin-Extramiana et al. 2017). Historically a sought after recreational and commercial fisheries species, giant sea bass experienced severe population declines in the USA due to overfishing in the early 20th century (Baldwin & Keiser 2008, Allen 2017, Ramírez-Valdez et al. 2021). Despite near extirpation in California, recent scientific evidence suggests that they are recovering after implementation of fishing regulations that decreased intentional and incidental catch of the species in the USA (Pondella & Allen 2008, Allen & Andrews 2012, House et al. 2016).

Due to their relative rarity, studies on giant sea bass are scarce and knowledge of their trophic ecology is largely limited to qualitative natural history reports (Young 1969, Feder et al. 1974, Domeier 2001). Giant sea bass are assumed to be generalist, high trophic level predators that feed on a wide array of primarily benthic nearshore rocky reef and kelp forest species, ranging from stingrays and small sharks to lobsters and octopuses (Domeier 2001, Allen & Andrews 2012, House et al. 2016). They are suction feeders, rapidly expanding their jaws to create a flow of water into their mouths that carries their prey along with it (Bishop et al. 2008). One of the only efforts to study giant sea bass diets compiled observations of individuals from the young-of-the-year age class and found that mysid shrimp are their dominant prey source (Benseman et al. 2019). Little else is known about their feeding ecology. For instance, little is known of the influence of ontogeny, different primary producers, or individual prey species on adult giant sea bass trophic dynamics. This study gathers baseline information that supports efforts aimed at anticipating broader ecosystem responses to the recent growth of giant sea bass populations in southern California.

Understanding how giant sea bass rely on different primary producers in their environment can help determine the extent to which shifts in production dynamics, whether from natural or anthropogenic drivers, might mediate population recovery. Kelp forests are key habitat for giant sea bass (Domeier 2001, House et al. 2016, Clevenstine & Lowe 2021). Kelp supports complex trophic systems by serving as an ecosystem engineer, creating structure and habitat in nearshore environments for diverse communities of organisms (Teagle et al. 2017, Layton et al. 2019). Primary production in kelp forest systems is derived chiefly from macroalgae (e.g. giant kelp *Macrocystis pyrifera*) and phytoplankton (Duggins et al. 1989, Fredriksen 2003, von Biela et al. 2016). Fluctuations in these producers can propagate throughout the food web, influencing the growth and production of higher trophic level species, including fishes (Koenigs et al. 2015, von Biela et al. 2016). Kelp forests globally are declining in patch size and kelp density, likely due to anthropogenic drivers of global change (Johnson et al. 2011, Steneck & Johnson 2014, Krumhansl et al. 2016, Layton et al. 2019). Threats to this critical habitat could hinder the ongoing recovery of giant sea bass, though our understanding of their reliance on kelp forests as producers is limited. While previous studies have demonstrated that, generally, higher trophic level fish tend to rely more on macroalgae-derived primary production in kelp forest ecosystems (Koenigs et al. 2015, von Biela et al. 2016), no studies have assessed the link between primary producers and giant sea bass trophic ecology.

Two commonly used tools to investigate trophic ecology are gut content analysis and stable isotope analysis. Gut contents provide information on what an organism was eating just before being sampled and are useful because they provide direct observations of different prey. Stable isotopes constitute a representation of what an organism eats that is integrated through space and time, depending on how quickly their tissues turnover. Ratios of nitrogen isotopes ($^{15}N/^{14}N$) can help determine the relative trophic position of an organism, because they enrich at a predictable rate with each increasing trophic level (Finlay et al. 2002, Post 2002). Ratios of carbon isotopes ($^{13}C/^{12}C$) tend to reflect sources of primary productivity, because carbon isotopic signatures are generally well conserved through trophic transfer (Hobson 2005, Kurle et al. 2011). Bulk ratios of carbon and nitrogen isotopes can be used to test for size/age-based differences in diet, incorporated into stable isotope mixing models to determine the relative contribution of different primary producers to the diet of a predator, and compared against each other to determine the isotopic niche of an organism (as a proxy for trophic niche). Compound specific stable isotope analysis of amino acids (CSIA-AA) splits bulk nitrogen into target amino acids that show different enrichment properties (Whiteman et al. 2019). By comparing these different amino acids, it is possible to get an estimate of the trophic position of an animal from a single sample of their tissue.

In this study, we leveraged bulk and compound specific stable isotope analyses along with gut content data to better understand the trophic role of a recovering predator, the giant sea bass. In particular,

we set out to determine (1) what giant sea bass eat, and how that changes as a function of size/ontogeny; (2) which primary production sources giant sea bass are most reliant on and if/how that relationship changes throughout their life history; (3) the relative trophic position of giant sea bass; and (4) what insight this information can give us about the role of giant sea bass in one of their key habitats, the kelp forest ecosystem.

2. MATERIALS AND METHODS

2.1. Sample collection

We collected fin clip samples — approximately 1 to 2 cm of tissue clipped from the anal fin — to perform stable isotope analyses. Typically, stable isotope analyses of fish use muscle tissue; however, previous studies have demonstrated that fin clips are good analogs for muscle tissue when the latter is not available, as was the case in this study (Suzuki et al. 2005, Sanderson et al. 2009, Hanisch et al. 2010, Jardine et al. 2011). Sampling took place from 2017 to 2020, and spanned the core range of giant sea bass, which is south of Pt. Conception, California, along the Pacific coast of Baja California and the upper Gulf of California, Mexico (Domeier 2001, Ramírez-Valdez et al. 2021) (Fig. 1). Most of our samples (n = 56) came from individuals caught by fishing cooperatives involved in the finfish fishery in Baja California, through a collaboration with the biological monitoring program, Proyecto Mero Gigante, and the non-profit Comunidad y Biodiversidad A.C. (COBI). The Mexico sampling locations ranged from predominantly soft bottom to predominantly rocky reef habitats and varied in the presence of kelp (Table S1 in the Supplement at www.int-res.com/articles/suppl/m695p157_supp.pdf). Additionally, we collected samples from La Jolla, California, as part of a separate effort permitted by the California Department of Fish and Wildlife (CDFW) that involved tagging and releasing giant sea bass (n = 5). We opportunistically collected 2 samples from deceased individuals that washed up in Solana Beach and Carlsbad, California. All USA sampling locations were near or within rocky reef and kelp forest areas with adjacent sandy bottom habitats. Stable isotope samples are typically preserved by freezing, but due to limited availability of freezer facilities for our samples from Mexico, we preserved all the fin clip samples in a 95% ethanol solution. Previous work investigating the impacts of different preservation methods on stable isotope analysis indicates ethanol preservation of fish tissues has minimal to no impact on isotope values (Sarakinos et al. 2002, Hetherington et al. 2019). In addition to fin clips, we gathered morphometric information on all the fish sampled, including total length (TL).

We gathered information on the isotopic signatures of potential primary producers (macroalgae vs. phytoplankton) through 2 methods. First, we collected samples of the dominant macroalgae (*Macrocystis pyrifera*) from a kelp forest in La Jolla (the same location where we collected La Jolla fin clip samples) in the fall of 2019 (n = 8). We also collected samples of pyrosomes (*Pyrosoma atlanticum*) from the offshore waters of San Diego, California, during Scripps Institution of Oceanography research cruises in the fall of 2019 (n = 10). Based on the distribution of *P. atlanticum* (O'Loughlin et al. 2020) and previous

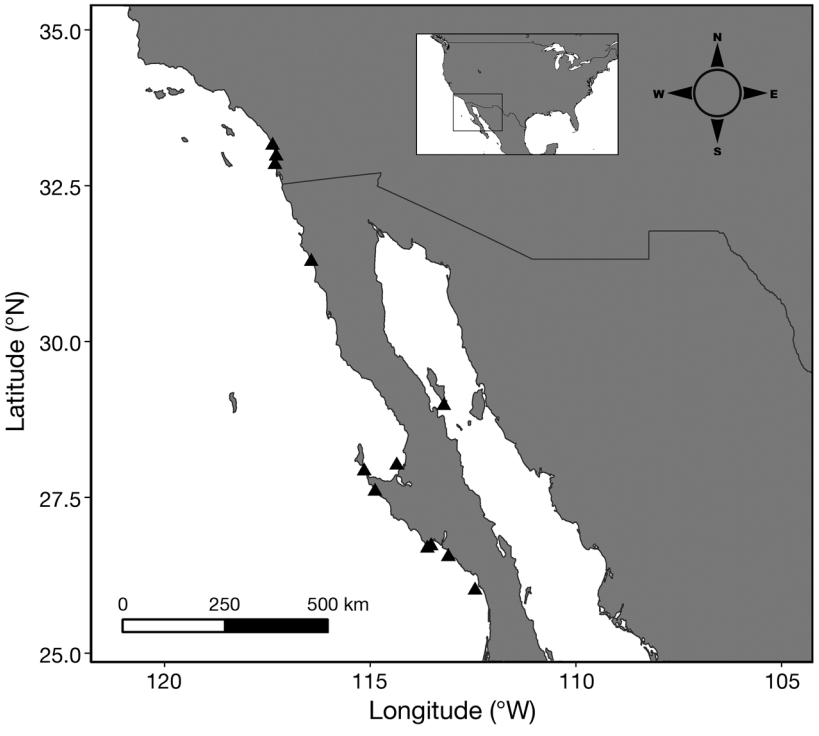

Fig. 1. Sampling locations (▲) for giant sea bass fin clips. From north to south these locations are: Carlsbad, Solana Beach, La Jolla, Ajusco Erendira, Bahia de Los Angeles, Guerrero Negro, Isla Natividad, Bahia Tortugas, Punta Abreojos, El Rosario, El Datil, Laguna San Ignacio, and San Juanico. The inset map places the study region into the context of broader continental North America

work using pyrosomes in isotope studies (Richards et al. 2020), we used our pyrosome samples as a primary consumer proxy for offshore phytoplankton production throughout our study region. We preserved these samples by freezing them. Second, we conducted a literature review and recorded *M. pyrifera* and particulate organic matter (POM; a proxy for phytoplankton) isotope values from studies that previously measured primary producers in our study region (Table S2) (Page et al. 2008, Hamilton et al. 2011, Vega-García et al. 2015, Piñón-Gimate et al. 2016, Kurle & McWhorter 2017, Gabara 2020).

2.2. Gut content data

Gut content data are difficult to collect for giant sea bass, because they are largely protected from harvest in the USA and those that are caught in fisheries are generally gutted at sea. To overcome this challenge and gather information on the diet of giant sea bass, we drew from multiple data sources. First, we conducted a literature review, recording all prey taxa mentioned and whether the observations were from live feeding events, from inspecting gut contents, or uncredited anecdotal reports. Second, the Hubbs-SeaWorld Research Institute (HSWRI) shared information recorded on the stomach contents of giant sea bass caught incidentally during their juvenile white seabass *Atractoscion nobilis* gill net surveys in the nearshore waters off San Diego county. Third, we conducted gut content analysis on 2 individuals that washed up in the San Diego region, 1 on Solana Beach and 1 on Mission Beach, California, as well as 10 individuals from Isla Natividad, Baja California that had their gut contents retained by fishing cooperative members on our request. And finally, we reached out to fellow researchers for any unpublished records of gut content analysis or observations of feeding interactions in the field (e.g. videos opportunistically taken by scuba divers). Most notably, Dr. Larry Allen provided information on an individual from La Jolla (L. G. Allen pers. comm.) that he had necropsied and gathered gut content from in 2015. After compiling the disparate records of stomach contents, we generated a list of potential prey items and grouped each based on our confidence in the source of the information.

2.3. Bulk stable isotope analysis

We prepared fin clip and primary producer samples for bulk stable isotope analysis in accordance with previously published works (Hanisch et al. 2010, Jardine et al. 2011, Hetherington et al. 2019). We removed each sample from its ethanol preservative (for fin clips) or the freezer (for primary producers), rinsed it with de-ionized water for at least 1 min, and freeze-dried for 48 h. Once dried, we homogenized the samples using a mortar and pestle and/or a scalpel and placed approximately 1 ± 0.2 mg (for fin clips) or 5 ± 0.2 mg (for primary producers) of material into pre-weighed tin capsules. The Isotope Biogeochemistry facility at Scripps Institution of Oceanography analyzed all samples to determine the bulk carbon and nitrogen isotope values. We expressed all results as δ values (parts per thousand differences from a standard or per mil; ‰) using the following equation:

$$\delta X = \left(\frac{R_{sample}}{R_{standard}} - 1\right) \times 1000 \quad (1)$$

where X is either ^{13}C or ^{15}N and R is the ratio $^{13}C/^{12}C$ or $^{15}N/^{14}N$ using acetanilide standards (Baker A068-03, Lot A15467).

2.4. Compound specific stable isotope analysis

We performed compound specific stable isotope analysis of amino acid (CSIA-AA) nitrogen on a subsample of 20 fin clips. The size of our subsample was dictated by the cost limitations of running CSIA-AA. We selected samples from Guerrero Negro, Mexico that represented a wide size range of fish (TL: 51 to 197 cm). We split a single fin clip from 1 individual into 3 subsamples that we processed separately to produce procedural reproducibility errors for each of 4 target AAs: alanine (Ala), glutamic acid (Glu), glycine (Gly), and phenylalanine (Phe). Ala and Glu are trophic AAs, meaning they enrich with rising trophic levels, while Gly and Phe are source AAs, meaning they do not enrich with rising trophic levels (Whiteman et al. 2019). The difference in enrichment between these AAs allows us to estimate the trophic position of an individual from a single sample (see Section 2.5.). The $\delta^{15}N$ of the selected AAs is not significantly altered by ethanol and thus preservation effects on trophic position estimation are negligible (Swalethorp et al. 2020).

We removed each sample from the ethanol preservative, rinsed it with de-ionized water for at least 1 min, and then freeze-dried for 48 h. We employed a relatively new high-precision method using high-pressure liquid chromatography and offline elemental analysis isotope ratio mass spectrometry (HPLC/

EA-IRMS) (Broek & McCarthy 2014, Swalethorp et al. 2020). All specifics of this method can be found in Swalethorp et al. (2020). Briefly, we hydrolyzed a minimum of 6 mg (dry weight) of each sample in 1 ml of 6 mol l^{-1} HCl in capped glass tubes for 24 h at 90°C. We then dried the samples on a centrifugal evaporator under vacuum at 60°C, re-dissolved them in 0.5 ml of 0.1 mol l^{-1} HCl, and filtered them through an IC Nillix — LG 0.2 µm hydrophilic polytetrafluoroethylene (PTFE) filter to remove particulates. Finally, we re-dried the samples before re-dissolving them in 100 µl of 0.1% trifluoroacetic acid (TFA) in Milli-Q water and transferring them to glass inserts in glass vials. We stored all samples at −80°C for 1 to 4 wk prior to AA purification. For each sample, we purified and collected the trophic AAs Ala and Glu, and the source AAs Gly and Phe. We dried these AAs in a centrifugal evaporator at 60°C, re-dissolved them in 40 µl of 0.1 mol l^{-1} HCl, then transferred them into small tin capsules and dried them under vacuum. We used the Stable Isotope Laboratory facility at the University of California, Santa Cruz to carry out analyses on a Nano-EA-IRMS designed for high precision analysis of low mass samples (≥0.6 µg N).

2.5. Data analysis

We performed all analyses using R statistical software, version 3.6.1 (R Core Team 2019). The code for our analyses can be found at https://github.com/kmblincow/GSBIsotopeAnalysis.

We analyzed the bulk stable isotope data for relationships with fish body size using Bayesian linear models coded in R and JAGS software (Plummer 2003) with the package R2jags (Su & Yajima 2020). To account for possible influences of year and sample location, we tested multiple models incorporating different combinations of these variables, including a derived categorical variable of year and sample site combined (see Table 1). We created the derived variable to address potential confounding changes in sites across years. We treated year, sample site, and the combined year and sample site variable as random effects, and the TL of each fish sampled as a fixed effect. We ran each model using 3 parallel Monte Carlo Markov Chain (MCMC) chains, each obtaining 350 000 samples, the first 25 000 of which were discarded as burn-in. We retained every 25th iteration to reduce autocorrelation, resulting in an output of 39 000 samples of the posterior distribution for each chain. We confirmed model convergence by evaluating trace plots and the potential scale reduction factor ($\hat{R}$) (Gelman & Rubin 1992). We used leave-one-out cross-validation (LOO) to determine which models best predicted the data using the package loo (Vehtari et al. 2017, 2020).

We evaluated the isotopic niche of different age classes of giant sea bass using the SIBER package (Stable Isotope Bayesian Ellipses in R) (Jackson et al. 2011). Giant sea bass are thought to mature between the ages of 7 and 13 (Domeier 2001, Hawk & Allen 2014). Using the age-growth equation derived by Hawk & Allen (2014), we calculated the expected age associated with each of our samples and classified them as either 'immature' (<7, n = 18), 'transition' (7 to 12, n = 23), or 'mature' (>12, n = 22). We calculated the standard ellipse area (SEAc), which is a representation of bivariate standard deviation, for each of these groups. Additionally, we performed Bayesian estimation of the standard ellipses and compared across groups. SEAc is robust to small sample sizes, unlike other isotopic niche metrics such as convex hulls (Jackson et al. 2011). We ran our SIBER model using 3 parallel MCMC chains, each obtaining 50 000 samples, the first 25 000 of which were discarded as burn-in. We retained every 5th iteration. We confirmed model convergence by evaluating trace plots and the potential scale reduction factor ($\hat{R}$).

We incorporated our bulk isotope results into a Bayesian isotope mixing model to determine what proportion of giant sea bass diets are derived from either phytoplankton or macroalgae primary production sources using the MixSIAR package (Stock et al. 2018). MixSIAR requires the input of source isotope values (i.e. macroalgae and phytoplankton primary production), mixture isotope values (i.e. giant sea bass), estimates of the trophic discrimination factors (TDF) between the source and mixture for each isotope, and data on relevant covariates (i.e. TL). We ran our model using 3 parallel MCMC chains, each obtaining 100 000 samples, the first 50 000 of which were discarded as burn-in. We retained every 50th iteration. We used the same convergence criteria as in the prior analyses.

To determine our source isotopic signatures, we collected the mean estimated bulk isotope values from multiple studies (including our own), and then calculated the mean and variance of these values. We subsequently used these means and variances as fixed source values (not estimated based on sample data) in our mixing model (Stock et al. 2018). We estimated the relative proportion of macroalgae-derived carbon by relying on isotopic estimates of the dominant Pacific coastal macroalgae species in our sam-

ple locations, *M. pyrifera* (Edwards & Hernández-Carmona 2005). However, we had 1 fin clip sample from the upper Gulf of California, which does not encompass the range of *M. pyrifera*. Despite the fact that other coastal macroalgae present in the upper Gulf of California likely have similar values to *M. pyrifera*, we chose to exclude this sample from the mixing model analysis because it was unreasonable to assume *M. pyrifera* would be contributing to its isotopic signature. To convert pyrosome isotope values into phytoplankton primary production (under the assumption that pyrosomes rely exclusively on a phytoplankton-derived food web), we corrected our pyrosome-derived $\delta^{15}N$ estimates by −2‰ and our $\delta^{13}C$ estimates by 0.5‰ based on previously published estimates of the trophic position of pelagic tunicates (Hetherington et al. 2018, Décima et al. 2019, Schram et al. 2020).

To our knowledge, there are no experimental estimates of TDF for giant sea bass. We chose to use mean TDF values of 0.9‰ (SD = 0.5) and 3.4‰ (SD = 0.5) for $\delta^{13}C$ and $\delta^{15}N$, respectively, based on previously published isotope research for similar species (Artero et al. 2015) and broad TDF estimates for carnivorous species (DeNiro & Epstein 1978, Post 2002). Since our source and mixture populations were multiple trophic steps apart, it was necessary to correct our TDF values based on that difference (Phillips et al. 2014). To do so we used the trophic position estimates from our CSIA-AA analysis (described below) to calculate a mean trophic position for giant sea bass and multiplied our TDF values by that value minus 1.

We used the 2 trophic (Trp) and 2 source (Scr) AA $\delta^{15}N$ values to calculate the trophic position of giant sea bass using β and TDF values from Bradley et al. (2015) and the following equation:

$$FCL = \frac{\delta^{15}N_{Trp} - \delta^{15}N_{Scr} - \beta}{TDF_{AA}} + 1 \quad (2)$$

where β is the $\delta^{15}N$ offset between Trp and Scr AAs in primary producers, while TDF_{AA} is the average $\delta^{15}N$ enrichment of Trp relative to Scr AAs in consumers for each increasing trophic step. To generate more robust trophic position estimates we used weighted means of both Ala and Glu, and Gly and Phe (Nielsen et al. 2015) and the following equation:

$$\delta^{15}N_{\bar{x}_W} = \frac{\sum \frac{\delta^{15}N_x}{\sigma_x^2}}{\sum \frac{1}{\sigma_x^2}} \quad (3)$$

where $\delta^{15}N_x$ is the value of a specific Trp or Scr AA and σ_x is the procedural reproducibility error reported here as the SD from replicate analysis of the 3 subsamples of 1 of the fin clips. These SD values were 0.24, 0.68, 0.17, 1.57 for Ala, Glu, Gly, and Phe, respectively. We also calculated weighted means for the β and TDF values and associated SDs (Bradley et al. 2015).

After calculating the trophic position associated with our samples, we performed a simple Bayesian linear regression to look for a relationship with fish size (TL) using the same model specifications described for the linear models above. For the fin clip sample that was split into 3 and run separately, we calculated the mean of the associated results so as not to triple count them.

3. RESULTS

3.1. Bulk stable isotopes

We gathered a total of 63 tissue samples from fish with TLs ranging from 44 to 197 cm (94.57 ± 42.08; mean ± SD). $\delta^{13}C$ values ranged from −16.50 to −12.39‰ (−14.53 ± 1.10; mean ± SD), and $\delta^{15}N$ values ranged from 15.95 to 19.54‰ (17.91 ± 0.90) (Fig. S1). Due to our opportunistic sampling, the sample sites are not evenly represented (Table S1), with the majority of samples coming from Baja California, Mexico (n = 56), in particular Guerrero Negro (n = 31). Our Bayesian linear models indicated a strong positive relationship between TL and $\delta^{13}C$ (Fig. 2a). LOO model comparison found that sample site and TL were the most important variables for predicting $\delta^{13}C$ (Table 1). While LOO identified year and TL as the best predictors of $\delta^{15}N$ out of the variables we tested (Table 1), the relationship between TL and $\delta^{15}N$ was weak (Fig. 2b). We should note that some of the models we evaluated using LOO had a small number of Pareto *k* values that exceeded 0.5. We evaluated each of these points individually, and found that they rarely exceeded 0.7, the recommended cutoff for the utility of LOO methods in model comparison (Vehtari et al. 2017). Based on the guidance of Vehtari et al. (2017), we decided our models were robust for LOO comparison.

By plotting the SEAc derived from the SIBER analysis, we found overlap in the isotopic niches of the 3 different age groups (Fig. 3a). We found that the mature age class had the highest Bayesian SEAc estimate, followed by the transition, then the immature age classes (Fig. 3b).

Based on the literature values and our primary producer samples, we calculated $\delta^{13}C$ values (mean ±

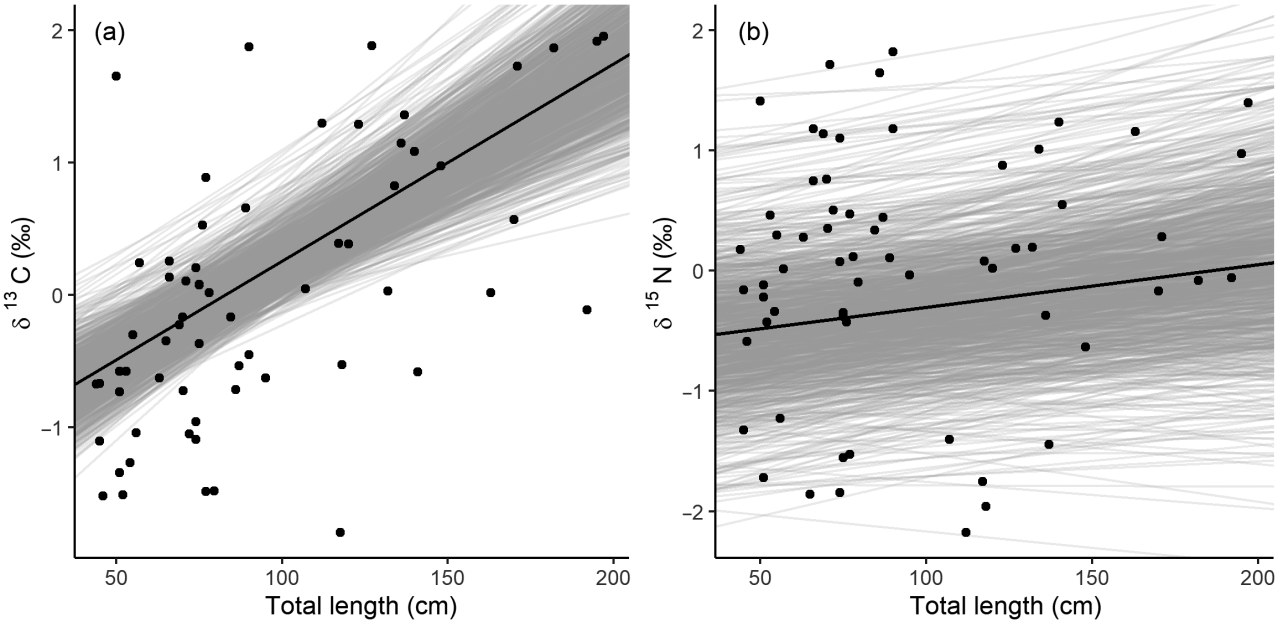

Fig. 2. Bayesian estimates of the linear relationships between the bulk isotope results and total length. Note that the *y*-axis displays the scaled bulk isotope values, which have a mean of 0 and SD of 1. Black lines: mean posterior hyperparameter estimate for the slope and intercept for each respective model; gray lines: 1000 random draws from the hyperparameter posterior distribution for the slope and intercept for each respective model; black dots: raw data points. (a) $\delta^{13}C$ and total length (cm) using the model which incorporated total length as a fixed effect and sample site as a random effect. (b) $\delta^{15}N$ and total length (cm) using the model which incorporated total length as a fixed effect and year as a random effect

SD) of −14.81 ± 0.58 and −21.55 ± 0.45, and $\delta^{15}N$ values of 9.46 ± 0.47 and 6.71 ± 0.39, for macroalgae and phytoplankton, respectively. When using these as our source values, the mixing model showed that giant sea bass are chiefly reliant on macroalgae as a basal carbon source and that this trend increases with size (Fig. 4). The median proportion of the diet associated with macroalgae was 0.61 (95% CI: 0.55–0.66) at the smallest end of the size range and 0.91 (95% CI: 0.83–0.95) at the largest end of the size range.

Table 1. Leave-one-out cross-validation model comparison testing the relationship between bulk isotope estimates and total length (TL; fixed effect), sample site (random effect), year (random effect), and year and site combined (YearSite; random effect). Expected log pointwise predictive accuracy (elpd_loo) is a measure of the predictive accuracy of the model which can be compared across models using the same data. The difference between these values for different models is given by the elpd_diff column, and the SE of component-wise differences of the elpd_loo between models is shown in the se_diff column

Isotope	Model	elpd_loo	elpd_diff	se_diff
$\delta^{13}C$	$\delta^{13}C$ ~ TL + Site	−77.8	0	0
	$\delta^{13}C$ ~ TL + YearSite	−77.9	−0.1	0.4
	$\delta^{13}C$ ~ TL	−77.9	−0.1	1.5
	$\delta^{13}C$ ~ TL + Year	−78.5	−0.7	1.6
	$\delta^{13}C$ ~ Year	−91.1	−13.3	5.8
	$\delta^{13}C$ ~ Site	−91.5	−13.7	5.8
	$\delta^{13}C$ ~ YearSite	−91.5	−13.7	5.8
$\delta^{15}N$	$\delta^{15}N$ ~ TL + Year	−86.0	0	0
	$\delta^{15}N$ ~ Year	−86.3	−0.3	1.1
	$\delta^{15}N$ ~ TL + YearSite	−89.4	−3.4	2.6
	$\delta^{15}N$ ~ TL + Site	−89.6	−3.6	3.3
	$\delta^{15}N$ ~ YearSite	−90.1	−4.2	2.7
	$\delta^{15}N$ ~ Site	−90.6	−4.6	3.6
	$\delta^{15}N$ ~ TL	−91.1	−5.2	4.1

3.2. CSIA-AA

Of the 20 samples we used for CSIA-AA, we found that 3 had unreasonably high Phe $\delta^{15}N$ values that led to very low trophic position estimates, and none of these were supported by the associated bulk $\delta^{15}N$ data. These samples had possibly degraded and were classified as outliers and subsequently removed from further analyses (Fig. S2). Additionally, we were unable to determine the Gly value for 1 sample, so we did not include that sample in our trophic position estimates. Ala values ranged from 25.65 to 30.06‰ (28.04 ±

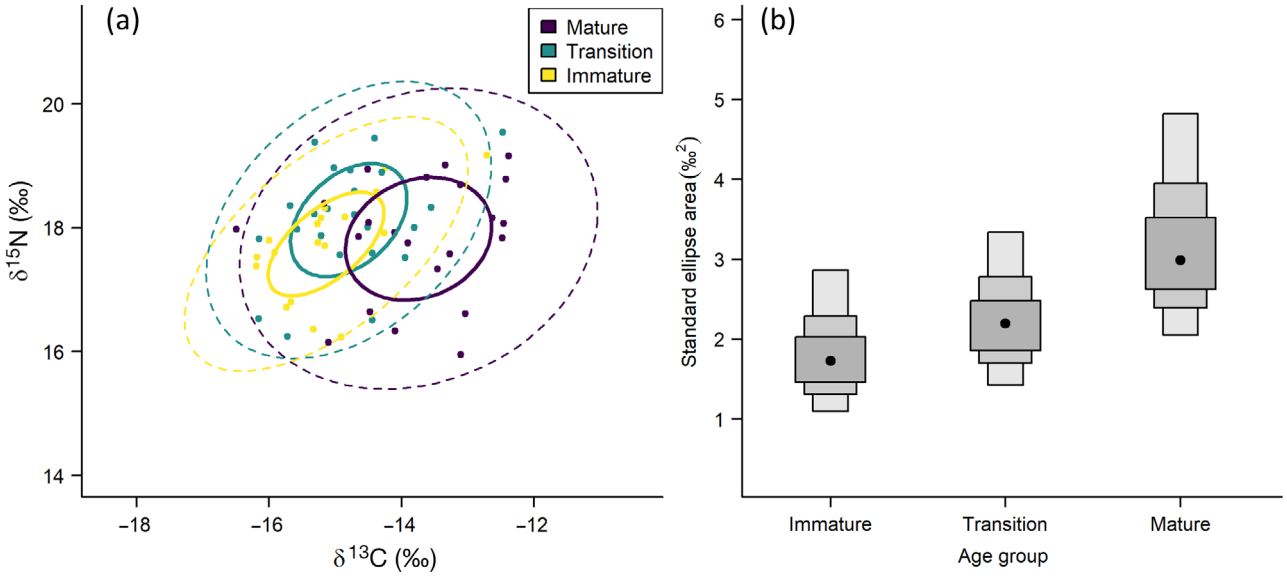

Fig. 3. Results of the SIBER analysis. (a) Bulk stable isotope biplot with standard ellipse areas (SEAc) for each age class (solid ellipses), and ellipses encompassing 95% of the data (dotted lines). (b) Bayesian estimates of the SEAc with (black dot) the mode and (boxes) the 50%, 75%, and 95% credible intervals

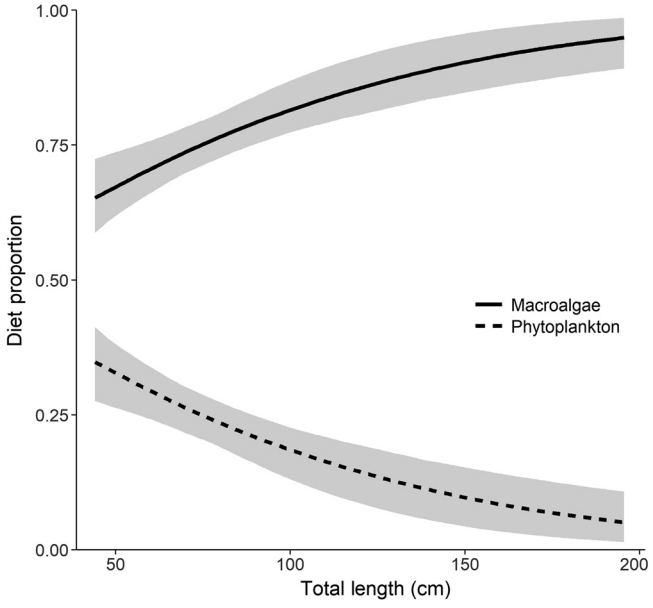

Fig. 4. Mixing model results showing the relative proportion of different primary producers in giant sea bass diets as a function of total length. Solid and dashed lines: posterior medians; gray shaded areas: 95% credible intervals

1.45), Glu values ranged from 26.65 to 32.11‰ (29.81 ± 1.72), Gly values ranged from 7.15 to 11.51‰ (9.42 ± 1.00), and Phe values ranged from 10.01 to 13.16‰ (11.67 ± 0.90) (Fig. 5a). The trophic position estimates ranged from 2.7 to 4.1 (3.39 ± 0.35). We found a strong positive linear relationship between trophic position and TL (Fig. 5b).

3.3. Gut contents

Synthesizing information from the compiled gut content data and literature reports, we found a total of 36 prey items, 25 of which were associated with direct observations from giant sea bass ranging in size from 43.7 to 141.3 cm TL (77.93 ± 26.99, n = 23) (Table 2). Most of our gut content data did not include records of prey size, though where it was recorded, we found that the largest prey items tended to be associated with larger giant sea bass. We should note that this relationship was not reciprocal, and larger giant sea bass also had smaller prey items in their stomachs, such as the Solana Beach individual (137.0 cm TL) that had 20 individual crabs in its stomach ranging in size from 4.2 to 9.0 cm in carapace width. The gut contents revealed prey groups that were wide ranging in terms of life history strategies, habitat preferences, and predator-avoidance mechanisms. For example, we found fast-moving pelagic prey, such as sardines and market squid, alongside benthic prey that rely heavily on camouflage, such as turbots and octopus. Directly observed prey items included both fish (60%) and invertebrates (40%). Among directly observed fish prey, 10 different orders were represented, with no clear dominant group (1 to 2 species represented in each order). Among directly observed invertebrate prey, Decapoda was the dominant order, representing 60% of the species. Most directly observed prey were associated with benthic habitats (87.5%), with

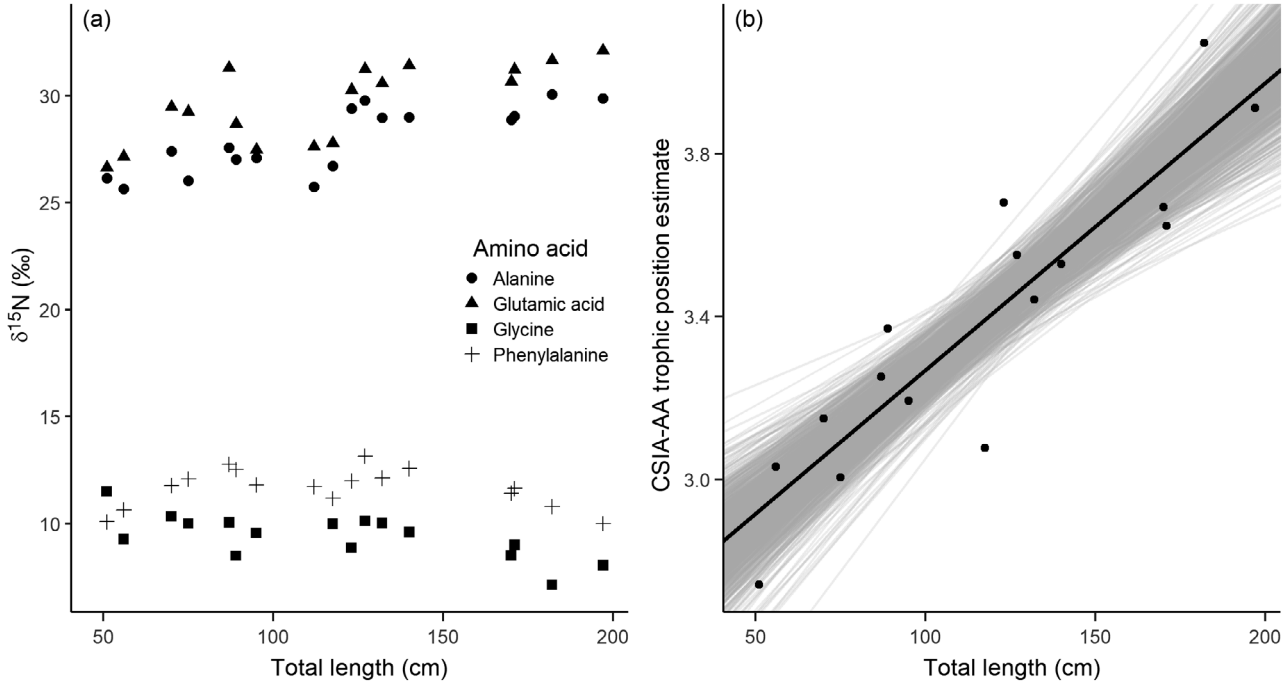

Fig. 5. Compound specific stable isotope analysis of amino acids (CSIA-AA) results. (a) The $\delta^{15}N$ values for the amino acids we tested. Glutamic acid and alanine are trophic amino acids which enrich with trophic level increases, while glycine and phenylalanine are source amino acids which do not enrich with increasing trophic levels. We used the differences between the source and trophic amino acids to estimate the trophic position for each fish tested using CSIA-AA. (b) The Bayesian estimate of the linear relationship between the trophic position and total length of samples analyzed using CSIA-AA. Black lines: mean posterior hyperparameter estimate for the slope and intercept for each respective model; gray lines: 1000 random draws from the hyperparameter posterior distribution for the slope and intercept for each respective model; black dots: raw data points

the largest proportion (58.3%) associated primarily with sandy bottom habitats. Other represented habitats included rocky or sandy bottom habitats (16.7%), rocky bottom habitats (12.5%), and pelagic habitats (12.5%).

4. DISCUSSION

As Critically Endangered (Cornish 2004) predators whose populations are beginning to recover, giant sea bass present an opportunity to learn how the return of generalist predator populations can influence the broader ecosystems to which they belong. Using stable isotopes, we demonstrated that adult giant sea bass continue to undergo shifts in their diet as they grow — relying more heavily on macroalgae-derived carbon, occupying higher trophic positions, and expanding their trophic niche with increasing size. Compiling available gut content records, we found that they consume a remarkably wide range of prey, consisting of a diverse assortment of primarily benthic-associated fish and invertebrate species. These findings lay the groundwork for understanding how giant sea bass recovery will influence kelp forest ecosystems and vice versa.

In addition to confirming long-held assumptions regarding giant sea bass trophic ecology, our study also uncovers some of the nuances underlying those assumptions. The wide array of observed prey supports the previous characterization of giant sea bass as generalist predators (Domeier 2001, Allen & Andrews 2012, House et al. 2016). Our trophic position estimates were relatively high, though not as high as those predicted from standardized trophic models. For example, FishBase estimates the trophic position of giant sea bass to be 4.5, while our mean estimate was 3.39 (Froese et al. 2022). The fact that these predators feed throughout the food web, including on low trophic level species (e.g. razor clams), results in a lower mean trophic position than predicted by standardized models. We think this also accounts for the weak relationship we found between bulk nitrogen and total length.

We found a relatively high overlap of trophic niche among age classes, though the mature age class had the largest trophic niche width. This suggests that while giant sea bass consume similar prey across size

Table 2. Prey types gathered from direct and anecdotal observations. The size of the giant sea bass (GSB) and associated prey items are given where available, along with the habitat associated with the prey type, and the source of the observation. Lengths of prey items are recorded in total length for fish, octopus, and squid, carapace width for crabs, and carapace length for other crustaceans. HSWRI: Hubbs-SeaWorld Research Institute; NA: not available. See Section 2.2 for details on the sources of data

	Type	Order	Common name	Scientific name	Habitat	Prey length (cm)	GSB total length (cm)	Source
Direct observation								
1	Fish	Ophidiiformes	Spotted cusk eel	*Chilara taylori*	Sandy	21.3	60.9	HSWRI
2	Fish	Batrachoidiformes	Plainfin midshipman	*Porichthys notatus*	Sandy	18	63.0	Isla Natividad, stomach
3	Fish	Pleuronectiformes	Hornyhead turbot	*Pleuronichthys verticalis*	Sandy	15.1; 15.9	63.3	HSWRI
4	Fish	Scorpaeniformes	Scorpionfish	*Scorpaenidae* spp.	Rocky	17.8	69.1	HSWRI
5	Fish	Clupeiformes	Pacific sardine	*Sardinops sagax*	Open water	NA	76.5	HSWRI; Feder et al. (1974); Baldwin & Keiser (2008)
6	Fish	Scorpaeniformes	Cabezon	*Scorpaenichthys marmoratus*	Rocky/sandy	21.6; 27.0	78.8	HSWRI
7	Fish	Istiophoriformes	Barracuda	*Sphyraena argentea*	Open water	NA	79.0	HSWRI
8	Fish	Batrachoidiformes	Specklefin midshipman	*Porichthys myriaster*	Rocky/sandy	NA	79.1	HSWRI; Young (1969); Baldwin & Keiser (2008)
9	Fish	Pleuronectiformes	Turbot	Unspecified	Sandy	NA	79.1	HSWRI
10	Fish	Acanthuriformes	Queenfish	*Seriphus politus*	Sandy	21.3	88.8	HSWRI
11	Fish	Rhinopristiformes	Shovelnose guitarfish	*Rhinobatos productus*	Sandy	30.0; 60.0	141.3	L. G. Allen, necropsy
12	Fish	Acanthuriformes	White croaker	*Genyonemus lineatus*	Sandy	18.3; NA	53.7; 86.7	HSWRI; Young (1969); Baldwin & Keiser (2008)
13	Fish	Uranoscopoidei	Smooth stargazer	*Kathetostoma averruncus*	Sandy	22	NA	SIO vertebrate collection
14	Fish	Myliobatiformes	Bat ray	*Myliobatis californica*	Rocky/sandy	NA	NA	Diver video
15	Invertebrate	Decapoda	Ghost shrimp	*Neotrypaea* spp.	Sandy	NA	42.1	HSWRI
16	Invertebrate	Octopoda	California two-spot	*Octopus bimaculoides*	Rocky	18	63.0	Isla Natividad, stomach
17	Invertebrate	Adapedonta	Razor clam	*Tagelus* spp.	Sandy	NA	79.1	HSWRI
18	Invertebrate	Decapoda	Spiny lobster	*Panulirus interruptus*	Rocky	NA	113.5	HSWRI; diver observation; Feder et al. (1974); Domeier (2001); Baldwin & Keiser (2008)
19	Invertebrate	Decapoda	Graceful crab	*Metacarcinus gracilis*	Sandy	8.0; 8.4; 9.0	137.0	Solana Beach, stomach
20	Invertebrate	Decapoda	Armed box crab	*Platymera gaudichaudii*	Sandy	4.2; 5.4; 6.3; 6.5; 6.6; 7.0; 7.0; 7.1; 7.2; 7.3; 7.4; 7.6; 7.7	137.0	Solana Beach, stomach
21	Invertebrate	Decapoda	Swimming crab	*Portunus xantusii*	Sandy	6.1; 6.2; 6.3; 6.8	137.0	Solana Beach, stomach
22	Invertebrate	Octopoda	Octopus	Unspecified	Rocky	NA	43.7; 46.6; 51.8; 61.5	HSWRI; Domeier (2001)
23	Invertebrate	Decapoda	Red crab	*Pleuroncodes planipes*	Rocky/sandy/ open water	NA	85.0; 110.0	Isla Natividad, stomach; Domeier (2001); Baldwin & Keiser (2008)
24	Invertebrate	Stomatopoda	California mantis shrimp	*Hemisquilla californiensis*	Sandy	7.0; NA	90.0; 141.3	Isla Natividad, stomach; L. G. Allen, necropsy
25	Invertebrate	Myopsida	Market squid	*Doryteuthis opalescens*	Open water	25.0; 22.4; 21.0	71.0	Mission Beach, stomach; Feder et al. (1974); Domeier (2001); Baldwin & Keiser (2008)
Anecdotal observation								
26	Fish	Perciformes	Pacific sargo	*Anisotremus davidsonii*	Rocky/sandy	NA	NA	Domeier (2001)
27	Fish	Perciformes	Ocean whitefish	*Caulolatilus princeps*	Rocky	NA	NA	Young (1969); Domeier (2001); Baldwin & Keiser (2008)
28	Fish	Ovalentaria	Blacksmith	*Chromis punctipinnis*	Rocky	NA	NA	Domeier (2001)
29	Fish	Clupeiformes	Northern anchovy	*Engraulis mordax*	Open water	NA	NA	Young (1969); Baldwin & Keiser (2008)
30	Fish	Perciformes	Kelp bass	*Paralabrax clathratus*	Rocky/sandy	NA	NA	Feder et al. (1974); Domeier (2001)
31	Fish	Perciformes	Barred sand bass	*Paralabrax nebulifer*	Sandy	NA	NA	Young (1969); Domeier (2001); Baldwin & Keiser (2008)
32	Fish	Scombriformes	Pacific bonito	*Sarda chiliensis lineolata*	Open water	NA	NA	Feder et al. (1974); Baldwin & Keiser (2008)
33	Fish	Scombriformes	Pacific mackerel	*Scomber japonicus*	Open water	NA	NA	Baldwin & Keiser (2008)
34	Fish	Labriformes	California sheephead	*Semicossyphus pulcher*	Rocky	NA	NA	Young (1969); Domeier (2001); Baldwin & Keiser (2008)
35	Fish	Carangiformes	Pacific jack mackerel	*Trachurus symmetricus*	Open water	NA	NA	Young (1969); Baldwin & Keiser (2008)
36	Fish	Myliobatiformes	Sting ray	Unspecified	Sandy	NA	NA	Domeier (2001); Baldwin & Keiser (2008)

ranges, the mature age class is interacting with the prey base in a different way. Explanations for the expansion of trophic niche width among the mature age class include an increased diversity of prey items available, individual specialization due to prey selection, or individual specialization due to spatial or temporal variability in prey (Matich et al. 2011). It is possible that size limitation influences the diversity of prey available across age classes. For the gut content samples where prey size information was available, larger prey items tended to be found in stomachs of larger individuals. For example, one of the largest giant sea bass sampled, measuring 141 cm in TL, had 2 shovelnose guitarfish *Rhinobatos productus* measuring 60 and 30 cm in TL inside its stomach. It is unlikely giant sea bass at the smaller end of those analyzed in this study (~40 to 60 cm) would be able to consume these prey. However, a separate large individual (137 cm TL) had 20 relatively small crabs in its stomach, ranging in carapace width from 4.2 to 7.7 cm. This suggests that size limitation might not be the sole driver of the increase in trophic niche width, and further study is warranted to investigate the role of individual specialization in the trophic ecology of mature giant sea bass.

One goal of this study was to determine which primary production sources giant sea bass rely on and whether that changes throughout their life history. Our mixing model results indicated that they feed chiefly in macroalgae-based food chains, and that this becomes increasingly true as they grow, shifting from ~60% macroalgae-derived carbon to ~90% across the size range studied. Anecdotal reports suggest smaller giant sea bass rely more heavily on pelagic species such as anchovies and sardines (Baldwin & Keiser 2008). Our limited records of pelagic prey items were associated with smaller individuals (76.5 and 79.0 cm in TL). This could account for the shifts we see in the relative proportion of primary producer sources in giant sea bass diets. Transient, pelagic-associated prey could serve as links between offshore and nearshore environments, increasing the relative proportion of phytoplankton-derived carbon in the tissue of smaller individuals. As giant sea bass grow and transition to a diet consisting of predominantly benthic organisms, there is an increase in the proportion of macroalgae-derived carbon in their diets. Previous studies tracing primary producer contributions to fish diets in nearshore environments in the eastern Pacific also document high proportions of macroalgae-derived carbon (Duggins et al. 1989, Koenigs et al. 2015, von Biela et al. 2016). The vast majority of the prey items we documented lived in benthic habitats, and most of those benthic prey were associated with sandy bottom habitats in particular. Initially, this might seem to contradict the mixing model results; however, sandy bottom habitats adjacent to kelp forests have been shown to rely significantly on primary production from drift macroalgae (Polis et al. 1997, Harrold et al. 1998, Crawley et al. 2009, Filbee-Dexter et al. 2018). It is likely that giant sea bass feed in sandy bottom habitats that rely on macroalgae from adjacent rocky reefs to subsidize their carbon supply. Indeed, studies investigating giant sea bass movement and anecdotal reports from diving and fishing communities suggest that they frequent areas where reef transitions to sandy bottom habitat (Burns et al. 2020, Clevenstine & Lowe 2021, K. M. Blincow unpubl. data).

It is unclear how current threats to kelp forest systems will influence the trophic ecology of giant sea bass and by extension their continued recovery, but we can speculate based on the results of this study. While the individuals in our analysis showed that a large portion of their diet is derived from macroalgae-based food chains, their prey are not necessarily obligate kelp forest inhabitants and neither are the giant sea bass themselves. Assuming that the ecosystem can still support an adequate prey supply, the potential negative impacts of kelp forest declines on giant sea bass might not be as severe as initially thought. One study that looked at the impact of *Macrocystis pyrifera* deforestation caused by urchin grazing on kelp forest food web structure found that the negative impacts of deforestation were not as strong at higher trophic levels similar to those occupied by giant sea bass (Graham 2004). Furthermore, a portion of the geographic range of giant sea bass does not coincide with the range of kelp (Ramírez-Valdez et al. 2021), and there are anecdotal reports of the local extirpation of kelp from rocky reefs in the Channel Islands having no apparent influence on their presence (Domeier 2001). These findings suggest that threats to kelp forests do not necessarily equate to threats to giant sea bass.

It is likely that the reason giant sea bass are often associated with kelp forest environments is the ability of these systems to support a high biomass of diverse prey groups, both in the immediate rocky reef environment and in adjacent sandy bottom habitats (Polis et al. 1997, Graham 2004). As such, the impact of the potential loss of kelp forests on giant sea bass will depend, at least in part, on the extent of the impacts on their prey. Generally, resource-limited conditions, like those brought on by the loss

of kelp, lead to increased diet specialization among predator populations because there is an increased need for efficient resource exploitation (Bolnick et al. 2003, Matich et al. 2011). For example, sea otters in Central California, a relatively resource-limited environment experiencing ongoing declines in kelp biomass, have more specialized diets when compared to sea otters in Washington (Laidre & Jameson 2006, Matich et al. 2011). It is possible that we could see a similar shift in giant sea bass trophic ecology with the reduction of kelp. Overall, their ability to exploit a diverse array of prey items suggests that giant sea bass populations will be able to adapt relatively well to changing conditions when compared to other more specialist predators.

Giant sea bass have been essentially absent from kelp forests in the USA for much of the 20th century, making it difficult to predict how their recovery will influence these ecosystems. It is very possible that ecosystem conditions have changed since the last time giant sea bass were a regular feature of these kelp forest environments. As generalists, their impact is spread across a wide variety of prey. They appear to feed on both fish and invertebrate species, but among invertebrate communities, species from the order Decapoda were most commonly targeted. These findings are similar to what has been found for goliath grouper *Epinephelus itajara*, an Atlantic large-bodied generalist predator that is also recovering from severely reduced population sizes due to overharvest (Koenig et al. 2020). Research on the diet of goliath grouper has found that they feed chiefly on crustaceans and benthic fish, targeting prey throughout the food web (Koenig et al. 2020). We found that giant sea bass also primarily feed on benthic species across different trophic levels. This suggests their recovery could have top down impacts on the structure of benthic communities in particular; however, the extent of these impacts is difficult to ascertain and further research and careful consideration is needed to fully characterize them. The dangers of misrepresenting these effects can be seen in the case of goliath grouper, where misconceptions regarding the trophic impacts of the species on fisheries species has been used to promote the cessation of conservation efforts (Koenig et al. 2020).

Further work expanding upon the foundation presented here would help inform our understanding of giant sea bass as well as the broader impacts of predator recovery. For example, measuring isotopic signatures from multiple tissue types with different turnover rates from the same individual would help tease apart the underlying mechanism of the growth in niche width we observed in mature age classes. Continuing to compile gut content data would support a more comprehensive understanding of giant sea bass prey communities, including primary prey species. Obtaining isotopic signatures of dominant prey species would help contextualize our results in terms of the broader food web and help confirm our assertion that giant sea bass rely on adjacent macroalgae-subsidized sandy bottom areas as feeding habitat. Pairing these suggested inquiries into the trophic ecology of giant sea bass with long-term monitoring of kelp forest communities would help assess the role of this recovering apex predator within the broader ecosystem, including potential top down effects on prey communities.

Acknowledgements. We acknowledge the funding sources that contributed to this work: the Mia Tegner Memorial Fellowship, the SIO Center for Marine Biodiversity and Conservation Mentorship Program, the Women Divers Hall of Fame Marine Conservation Scholarship sponsored by the Rachel Morrison Memorial Fund, the PADI foundation (via A.R.V.), and the Link Family Foundation (via Dr. Phil Hastings). We acknowledge Youssef Doss, our undergraduate REU intern who helped prepare fin clip samples for bulk isotope analysis. We also acknowledge everyone who contributed to the data collection for this project, including the fishing cooperatives who allowed us to use samples from their catch, COBI, HSWRI, Dr. Larry Allen, and the SIO Vertebrate Collection. We also thank Dr. Peter Kuriyama, Dr. Sarah Mesnick, Dwight Hwang, Alex Israel, and the San Diego lifeguards, who all worked to notify us and provide access when giant sea bass washed up on the beach. Thank you to the 3 anonymous reviewers who provided valuable feedback.

LITERATURE CITED

Allen LG (2017) GIANTS! Or… The return of the kelp forest king. Copeia 105:10–13

Allen LG, Andrews AH (2012) Bomb radiocarbon dating and estimated longevity of giant sea bass (*Stereolepis gigas*). Bull South Calif Acad Sci 111:1–14

Artero C, Koenig CC, Richard P, Berzins R, Guillou G, Bouchon C, Lampert L (2015) Ontogenetic dietary and habitat shifts in goliath grouper *Epinephelus itajara* from French Guiana. Endang Species Res 27:155–168

Baldwin DS, Keiser A (2008) Giant sea bass, *Stereolepis gigas*. In: Larinto T (ed) Status of the Fisheries Report. California Department of Fish and Game. https://nrm.dfg.ca.gov/FileHandler.ashx?DocumentID=34430&inline

Benseman SA, Couffer MC, Allen LG (2019) Behavior of young-of-the-year giant sea bass, *Stereolepis gigas*, off the sandy beaches of southern California. Bull South Calif Acad Sci 118:79–86

Bishop KL, Wainwright PC, Holzman R (2008) Anterior-to-posterior wave of buccal expansion in suction feeding fishes is critical for optimizing fluid flow velocity profile. J R Soc Interface 5:1309–1316

Bolnick DI, Svanbäck R, Fordyce JA, Yang LH, Davis JM, Hulsey CD, Forister ML (2003) The ecology of individu-

als: incidence and implications of individual specialization. Am Nat 161:1–28

Bradley CJ, Wallsgrove NJ, Choy CA, Drazen JC, Hetherington ED, Hoen DK, Popp BN (2015) Trophic position estimates of marine teleosts using amino acid compound specific isotopic analysis. Limnol Oceanogr Methods 13: 476–493

Broek TAB, McCarthy MD (2014) A new approach to $\delta^{15}N$ compound-specific amino acid trophic position measurements: Preparative high pressure liquid chromatography technique for purifying underivatized amino acids for stable isotope analysis. Limnol Oceanogr Methods 12: 840–852

Burns ES, Clevenstine AJ, Logan RK, Lowe CG (2020) Evidence of artificial habitat use by a recovering marine predator in southern California. J Fish Biol 97: 1857–1860

Clevenstine AJ, Lowe CG (2021) Aggregation site fidelity and movement patterns of the protected marine predator giant sea bass (*Stereolepis gigas*). Environ Biol Fishes 104:401–417

Cornish A (2004) *Stereolepis gigas*. IUCN Red List of Threatened Species 2004:e.T20795A9230697, doi:10.2305/IUCN.UK.2004.RLTS.T20795A9230697.en

Crawley KR, Hyndes GA, Vanderklift MA, Revill AT, Nichols PD (2009) Allochthonous brown algae are the primary food source for consumers in a temperate, coastal environment. Mar Ecol Prog Ser 376:33–44

Dayton PK, Tegner MJ, Edwards PB, Riser KL (1998) Sliding baselines, ghosts, and reduced expectations in kelp forest communities. Ecol Appl 8:309–322

Décima M, Stukel MR, López-López L, Landry MR (2019) The unique ecological role of pyrosomes in the Eastern Tropical Pacific. Limnol Oceanogr 64:728–743

DeNiro MJ, Epstein S (1978) Influence of diet on the distribution of carbon isotopes in animals. Geochim Cosmochim Acta 42:495–506

Domeier ML (2001) Giant sea bass. In: Leet WS, Dewees CM, Klingbeil R, Larson EJ (eds) California's living marine resources: a status report. California Department of Fish and Game, Sacramento, p 209–211

Donohue I, Petchey OL, Kéfi S, Génin A, Jackson AL, Yang Q, O'Connor NE (2017) Loss of predator species, not intermediate consumers, triggers rapid and dramatic extinction cascades. Glob Change Biol 23: 2962–2972

Duggins DO, Simenstad CA, Estes JA (1989) Magnification of secondary production by kelp detritus in coastal marine ecosystems. Science 245:170–173

Edwards MS, Hernández-Carmona G (2005) Delayed recovery of giant kelp near its southern range limit in the North Pacific following El Niño. Mar Biol 147:273–279

Erauskin-Extramiana M, Herzka SZ, Hinojosa-Arango G, Aburto-Oropeza O (2017) An interdisciplinary approach to evaluate the status of large-bodied Serranid fisheries: The case of Magdalena-Almejas Bay lagoon complex, Baja California Sur, Mexico. Ocean Coast Manage 145: 21–34

Feder HM, Turner CH, Limbaugh C (1974) Observation on fishes associated with kelp beds in Southern California. Calif Fish Game Bull 160:1–144

Filbee-Dexter K, Wernberg T, Norderhaug KM, Ramirez-Llodra E, Pedersen MF (2018) Movement of pulsed resource subsidies from kelp forests to deep fjords. Oecologia 187:291–304

Finlay JC, Khandwala S, Power ME (2002) Spatial scales of carbon flow in a river food web. Ecology 83:1845–1859

Fredriksen S (2003) Food web studies in a Norwegian kelp forest based on stable isotope ($\delta^{13}C$ and $\delta^{15}N$) analysis. Mar Ecol Prog Ser 260:71–81

Froese R, Binohlan CB, Pauly D (2022) FishBase: *Stereolepis gigas* Ayres, 1859. https://www.fishbase.de/summary/3310

Gabara SS (2020) Trophic structure and potential carbon and nitrogen flow of a rhodolith bed at Santa Catalina Island inferred from stable isotopes. Mar Biol 167:30

Gelman A, Rubin DB (1992) A single series from the Gibbs sampler provides a false sense of security. In: Bernardo JM, Berger JO, Dawid AP, Smith AFM (eds) Bayesian statistics 4. Oxford University Press, Oxford, p 625–631

Graham MH (2004) Effects of local deforestation on the diversity and structure of southern California giant kelp forest food webs. Ecosystems 7:341–357

Hamilton SL, Caselle JE, Lantz CA, Egloff TL and others (2011) Extensive geographic and ontogenetic variation characterizes the trophic ecology of a temperate reef fish on southern California (USA) rocky reefs. Mar Ecol Prog Ser 429:227–244

Hanisch JR, Tonn WM, Paszkowski CA, Scrimgeour GJ (2010) $\delta^{13}C$ and $\delta^{15}N$ signatures in muscle and fin tissues: nonlethal sampling methods for stable isotope analysis of salmonids. N Am J Fish Manage 30:1–11

Harrold C, Light K, Lisin S (1998) Organic enrichment of submarine-canyon and continental-shelf benthic communities by macroalgal drift imported from nearshore kelp forests. Limnol Oceanogr 43:669–678

Hawk HA, Allen LG (2014) Age and growth of the giant sea bass, *Stereolepis gigas*. CCOFI Rep 55:128–134

Heithaus MR, Frid A, Wirsing AJ, Worm B (2008) Predicting ecological consequences of marine top predator declines. Trends Ecol Evol 23:202–210

Hetherington ED, Seminoff JA, Dutton PH, Robison LC, Popp BN, Kurle CM (2018) Long-term trends in the foraging ecology and habitat use of an endangered species: an isotopic perspective. Oecologia 188:1273–1285

Hetherington ED, Kurle CM, Ohman MD, Popp BN (2019) Effects of chemical preservation on bulk and amino acid isotope ratios of zooplankton, fish, and squid tissues. Rapid Commun Mass Spectrom 33:935–945

Hobson KA (2005) Stable isotopes and the determination of avian migratory connectivity and seasonal interactions. Auk 122:1037–1048

House PH, Clark BLF, Allen LG (2016) The return of the king of the kelp forest: Distribution, abundance, and biomass of giant sea bass (*Stereolepis gigas*) off Santa Catalina Island, California, 2014–2015. Bull South Calif Acad Sci 115:1–14

Jackson AL, Inger R, Parnell AC, Bearhop S (2011) Comparing isotopic niche widths among and within communities: SIBER - Stable Isotope Bayesian Ellipses in R. J Anim Ecol 80:595–602

Jardine TD, Hunt RJ, Pusey BJ, Bunn SE (2011) A non-lethal sampling method for stable carbon and nitrogen isotope studies of tropical fishes. Mar Freshw Res 62:83–90

Johnson CR, Banks SC, Barrett NS, Cazassus F and others (2011) Climate change cascades: Shifts in oceanography, species' ranges and subtidal marine community dynamics in eastern Tasmania. J Exp Mar Biol Ecol 400:17–32

Koenig CC, Coleman FC, Malinowski CR (2020) Atlantic goliath grouper of Florida: to fish or not to fish. Fisheries (Bethesda, MD) 45:20–32

Koenigs C, Miller RJ, Page HM (2015) Top predators rely on carbon derived from giant kelp *Macrocystis pyrifera*. Mar Ecol Prog Ser 537:1–8

Krumhansl KA, Okamoto DK, Rassweiler A, Novak M and others (2016) Global patterns of kelp forest change over the past half-century. Proc Natl Acad Sci USA 113: 13785–13790

Kurle CM, McWhorter JK (2017) Spatial and temporal variability within marine isoscapes: implications for interpreting stable isotope data from marine systems. Mar Ecol Prog Ser 568:31–45

Kurle CM, Sinclair EH, Edwards AE, Gudmundson CJ (2011) Temporal and spatial variation in the $\delta^{15}N$ and $\delta^{13}C$ values of fish and squid from Alaskan waters. Mar Biol 158:2389–2404

Laidre KL, Jameson RJ (2006) Foraging patterns and prey selection in an increasing and expanding sea otter population. J Mammal 87:799–807

Layton C, Shelamoff V, Cameron MJ, Tatsumi M, Wright JT, Johnson CR (2019) Resilience and stability of kelp forests: the importance of patch dynamics and environment-engineer feedbacks. PLOS ONE 14:e0210220

Matich P, Heithaus MR, Layman CA (2011) Contrasting patterns of individual specialization and trophic coupling in two marine apex predators. J Anim Ecol 80:294–305

Nielsen JM, Popp BN, Winder M (2015) Meta-analysis of amino acid stable nitrogen isotope ratios for estimating trophic position in marine organisms. Oecologia 178: 631–642

O'Loughlin JH, Bernard KS, Daly EA, Zeman S, Fisher JL, Brodeur RD, Hurst TP (2020) Implications of *Pyrosoma atlanticum* range expansion on phytoplankton standing stocks in the Northern California Current. Prog Oceanogr 188:102424

Page HM, Reed DC, Brzezinski MA, Melack JM, Dugan JE (2008) Assessing the importance of land and marine sources of organic matter to kelp forest food webs. Mar Ecol Prog Ser 360:47–62

Phillips DL, Inger R, Bearhop S, Jackson AL and others (2014) Best practices for use of stable isotope mixing models in food-web studies. Can J Zool 92:823–835

Piñón-Gimate A, Gómez-Valdez MM, Mazariegos-Villarreal A, Serviere-Zaragoza E (2016) Trophic relationships between two gastropods and seaweeds in subtropical rocky reefs based on stable isotope analyses. J Shellfish Res 35:191–197

Plummer M (2003) JAGS: a program for analysis of Bayesian graphical models using Gibbs sampling. https://www.r-project.org/conferences/DSC-2003/Proceedings/Plummer.pdf

Polis GA, Anderson WB, Holt RD (1997) Toward an integration of landscape and food web ecology: the dynamics of spatially subsidized food webs. Annu Rev Ecol Syst 28: 289–316

Pondella DJ, Allen LG (2008) The decline and recovery of four predatory fishes from the Southern California Bight. Mar Biol 154:307–313

Post DM (2002) Using stable isotopes to estimate trophic position: models, methods, and assumptions. Ecology 83: 703–718

R Core Team (2019) R: a language and environment for statistical computing. R Foundation for Statistical Computing, Vienna

Ramírez-Valdez A, Rowell TJ, Dale KE, Craig MT and others (2021) Asymmetry across international borders: research, fishery and management trends and economic value of the giant sea bass (*Stereolepis gigas*). Fish Fish 22:1392–1411

Richards TM, Sutton TT, Wells RJD (2020) Trophic structure and sources of variation influencing the stable isotope signatures of meso- and bathypelagic micronekton fishes. Front Mar Sci 7:507992

Ritchie EG, Johnson CN (2009) Predator interactions, mesopredator release and biodiversity conservation. Ecol Lett 12:982–998

Sadovy de Mitcheson Y, Craig MT, Bertoncini AA, Carpenter KE and others (2013) Fishing groupers towards extinction: a global assessment of threats and extinction risks in a billion dollar fishery. Fish Fish 14: 119–136

Sanderson BL, Tran CD, Coe HJ, Pelekis V, Steel EA, Reichert WL (2009) Nonlethal sampling of fish caudal fins yields valuable stable isotope data for threatened and endangered fishes. Trans Am Fish Soc 138: 1166–1177

Sarakinos HC, Johnson ML, Vander Zanden MJ (2002) A synthesis of tissue-preservation effects on carbon and nitrogen stable isotope signatures. Can J Zool 80: 381–387

Schmitz OJ, Hawlena D, Trussell GC (2010) Predator control of ecosystem nutrient dynamics. Ecol Lett 13:1199–1209

Schram JB, Sorensen HL, Brodeur RD, Galloway AWE, Sutherland KR (2020) Abundance, distribution, and feeding ecology of *Pyrosoma atlanticum* in the Northern California Current. Mar Ecol Prog Ser 651:97–110

Steneck RS, Johnson CR (2014) Kelp forests: dynamic patterns, processes and feedbacks In: Burtness MD, Bruno J, Silliman BR, Stachowicz JJ (eds) Marine community ecology and conservation. Sinauer Associates, Sunderland, MA, p 315–336

Stock BC, Jackson AL, Ward EJ, Parnell AC, Phillips DL, Semmens BX (2018) Analyzing mixing systems using a new generation of Bayesian tracer mixing models. PeerJ 6:e5096

Su YS, Yajima M (2020) R2jags: Using R to Run 'JAGS'. https://cran.r-project.org/web/packages/R2jags/index.html

Suzuki KW, Kasai A, Nakayama K, Tanaka M (2005) Differential isotopic enrichment and half-life among tissues in Japanese temperate bass (*Lateolabrax japonicus*) juveniles: implications for analyzing migration. Can J Fish Aquat Sci 62:671–678

Swalethorp R, Aluwihare L, Thompson AR, Ohman MD, Landry MR (2020) Errors associated with compound-specific $\delta^{15}N$ analysis of amino acids in preserved fish samples purified by high-pressure liquid chromatography. Limnol Oceanogr Methods 18:259–270

Teagle H, Hawkins SJ, Moore PJ, Smale DA (2017) The role of kelp species as biogenic habitat formers in coastal marine ecosystems. J Exp Mar Biol Ecol 492:81–98

Vega-García PD, Piñón-Gimate A, Vélez-Arellano N, Lluch-Cota SE (2015) Differences in diet of green (*Haliotis fulgens*) and pink (*Haliotis corrugata*) wild abalone along the Pacific coast of the Baja California Peninsula, using stable isotope analyses. J Shellfish Res 34:879–884

Vehtari A, Gelman A, Gabry J (2017) Practical Bayesian model evaluation using leave-one-out cross-validation and WAIC. Stat Comput 27:1413–1432

Vehtari A, Gabry J, Magnusson M, Yao Y, Bürkner P, Paananen T, Gelman A (2020) loo: efficient leave-one-out

cross-validation and WAIC for Bayesian models. https://mc-stan.org/loo/

von Biela VR, Newsome SD, Bodkin JL, Kruse GH, Zimmerman CE (2016) Widespread kelp-derived carbon in pelagic and benthic nearshore fishes suggested by stable isotope analysis. Estuar Coast Shelf Sci 181: 364–374

Waterhouse L, Heppell SA, Pattengill-Semmens CV, McCoy C, Bush P, Johnson BC, Semmens BX (2020) Recovery of critically endangered Nassau grouper (*Epinephelus striatus*) in the Cayman Islands following targeted conservation actions. Proc Natl Acad Sci 117:1587–1595

Whiteman JP, Elliott Smith EA, Besser AC, Newsome SD (2019) A guide to using compound-specific stable isotope analysis to study the fates of molecules in organisms and ecosystems. Diversity (Basel) 11:8

Young PH (1969) The California partyboat fishery 1947–1967. Calif Dep Fish Game Fish Bull 145

Editorial responsibility: John Griffin, Swansea, UK
Reviewed by: L. G. Allen, C. Malinowski and 1 anonymous referee

Submitted: January 19, 2022
Accepted: July 5, 2022
Proofs received from author(s): August 18, 2022